3D registration using a new implementation of the ICP algorithm based on a comprehensive lookup matrix: application to medical imaging

Ahmad Almhdie, Christophe Léger, Mohamed Deriche, Roger Lédée

3D REGISTRATION USING A NEW IMPLEMENTATION OF THE ICP ALGORITHM BASED ON A COMPREHENSIVE LOOKUP MATRIX: APPLICATION TO MEDICAL IMAGING

Ahmad Almhdie[1], Christophe Léger[1,*], Mohamed Deriche[2], Roger Lédée[1]

[1] Laboratory of Electronics, Signals and Images (LESI),

University of Orléans, 12 rue de Blois, BP 6744, 45067 Orléans cedex 2, France

Tel: +33 238 494 563, Fax: +33 238 417 245

E-mails: {Ahmad.Almhdie, Christophe.Leger, Roger.Ledee}@univ-orleans.fr

[2] Electrical Engineering Department

King Fahd University of Petroleum and Minerals, P.O. Box 1427, Dhahran, 31261, Saudi Arabia

Tel: +966 3 860 1523, Fax: +966 3 860 3535

E-mail: mderiche@kfupm.edu.sa

[*]Corresponding author

ABSTRACT

The iterative closest point (ICP) algorithm is an efficient algorithm for robust rigid registration of 3D data. Results provided by the algorithm are highly dependent upon the step of finding corresponding pairs between the two sets of 3D data before registration. In this paper, a look up matrix is introduced in the point matching step to enhance the overall ICP performance. Convergence properties and robustness are evaluated in the presence of Gaussian and impulsive noise, and under different data set sizes. The new algorithm has been evaluated on 3D medical data. It has been applied successfully to register closed surfaces acquired using different medical imaging modalities.

Keywords: surface registration, ICP algorithm, point matching, medical data.

1. INTRODUCTION

The registration of 3D data sets is an important task in both Computer Vision and Photogrammetry, especially for satellite and air photography, or in the medical field. A detailed overview of image registration techniques can be found in (Zitová and Flusser, 2003). Medical diagnosis can be assisted using monomodal or multimodal image registration. In monomodal registration, data are obtained from a single imaging technique. The main interest of this mode is to highlight differences between the data registered: evolution or remission of a disease, impact of a treatment on a patient over a period of time, comparison of medical and reference data (atlas), etc. On the other hand, multimodal registration merges complementary information obtained from at least two imaging modalities of the same patient (Elsen et al., 1993). For example, (Kagadis et al., 2002) present a comparative study of surface registration of SPECT (Single Photon Emission Computed Tomography) images, which provide information about the functional activities of an organ, and CT (Computed Tomography) images, which offer organ anatomy description. In radiology, medical image registration is a visualisation tool which significantly facilitates the early detection of tumours and other diseases, and helps to improve the diagnosis accuracy (Kneuaorek et al., 2000). Registration is also used in functional analysis and surgical planning. It is employed in surgery to carry out a precise planning in order to prepare/or and simulate complex surgical procedures (Sylvain, 2000; Ourselin, 2002). Another application of registration in the medical field consists in reconstructing 3D models (Kneuaorek et al., 2000; Matabosch et al., 2005). It facilitates the acquisition of several views of the body to be digitized, and can also assist the use of atlas or normal or pathological data bases (Cuadra et al., 2004).

Different methods proposed for medical image registration have been discussed in (Maintz and Viergever, 1998; Wan and Li, 2003), with some targeting medical surface registration, such as in (Audette et al., 2000). Rigid surface registration is used for the determination of correspondence

functions between different sets of structured 3D data points representing the same surface. It gives the estimation of motion parameters that bring the two surfaces into alignment.

The iterative closest point (ICP) algorithm, originally proposed by (Besl and McKay, 1992), is one of the most popular methods used for estimating the rigid transformation of roughly aligned 3D data sets. It is widely used for the rigid registration of surfaces (Akca, 2004; Liu, 2004) when:

1. dense data is assumed,
2. a good initial estimate is available,
3. selected scene points from the scene surface have correspondences in the reference surface.

The most important step of the ICP algorithm consists in choosing corresponding (closest) points within the two 3D data sets. Since the accuracy of the search for correspondence points affects the estimation of the transformation parameters for registration, the output of this step has a major impact over the following stages, and influences the overall performance of the algorithm. This step depends upon both the selection of the points of the two surfaces, and the method used for finding the correspondence of the selected points. The Original ICP algorithm (Besl and McKay, 1992), denoted OICP in this paper, searches for the closest point in the reference surface for each point in the scene surface without any restrictions.

Widespread interest in 3D surface registration using the OICP algorithm has motivated the scientific community to propose new techniques for enhancing the different steps of the original algorithm. Many variants have been developed to speed up the convergence and/or improve the performance of the different phases of the algorithm. A good review of these variants can be found in (Rusinkiewicz and Levoy, 2001). There has been significant interest regarding the selection of points used for the estimation of transformation parameters. In (Chetverikov et al., 2002), the Trimmed ICP improves both the rapidity and the accuracy of the transformation parameter estimation by selecting only a predefined number of estimated matched pairs for the calculation of the ‘optimal motion’. Additional features, such as curvature and moment invariants, can also be used to improve the

correspondence search (Sharp et al., 2002; Bendels et al., 2004). However, in this paper, no additional information is assumed to be available for the correspondence search. The Picky ICP (Zinsser et al., 2003) rejects all points previously estimated to correspond to one reference point, except the one with the smallest distance. This approach reduces convergence problems that may arise using the original ICP algorithm, when a common reference point is assigned to multiple points in the scene surface. However, this affects the performance of the algorithm negatively in noisy situations, since many points are discarded in the estimation step.

Following (Rusinkiewicz and Levoy, 2001), different ICP variants can be classified according to six different criteria:

1) Selecting subsets from the given 3D data sets.
2) Finding correspondence points.
3) Weighting the estimated correspondence pairs.
4) Rejecting false matches.
5) Assigning an error metric.
6) Minimizing the error metric.

This paper focuses on the second part: the search for pair correspondences from the two 3D surface data sets. The aim is to enhance the performance of the correspondence search step of the OICP algorithm. In order to have a fair comparison, the OICP, PICP and CICP algorithms presented here differ only by this second correspondence search step. Here, we call PICP algorithm the OICP algorithm used with the Picky ICP method for finding correspondence points. The use of a new comprehensive look up matrix is investigated and evaluated. The proposed CICP (C for comprehensive) algorithm ensures unique matches of correspondence pairs.

The paper is organized as follows. First, the original OICP and PICP algorithms are summarized. The new CICP algorithm is then described and details of the performance analyses are given. In the following section, the performance improvement of the CICP algorithm is evaluated using medical

data. The new version of the algorithm is then used to register medical data from two different medical imaging modalities. Finally some concluding remarks are given.

2. OVERVIEW OF THE ICP ALGORITHM

2.1. OICP overview

Let us assume that the given two surfaces to be registered can be described as point sets; the scene data points, **P**, with N_p points, $\{p_i,\ i=1, \ldots, N_p\}$, and the reference data points, **M**, with N_m points, $\{m_j,\ j=1, \ldots, N_m\}$. Depending upon the sampling of the surfaces, N_p is not necessarily equal to N_m. Furthermore, the point p_i of the scene surface does not necessarily represent an exact 3D correspondence to the point m_i of the reference surface. However, the search space is determined by the size of the scene data set; i.e., N_p. The OICP algorithm can be summarized as follows:

A. Initialization:

1) Let the initial scene surface $\mathbf{P}_{0,}$ be equal to **P**.
2) Define the maximum number of iterations $\mathbf{k}_{max}$.
3) Initialize the translation vector and the rotation matrix as follows:

$$\mathbf{T} = \begin{bmatrix} t_1 \\ t_2 \\ t_3 \end{bmatrix} \quad \text{and} \quad \mathbf{R} = \begin{bmatrix} r_{11} & r_{12} & r_{13} \\ r_{21} & r_{22} & r_{23} \\ r_{31} & r_{32} & r_{33} \end{bmatrix} \tag{1}$$

with the initial coefficient of the translation vector and rotation matrix set as follows: $t_u = 0$, $r_{u,v} = 0$ if $u \neq v$, and $r_{u,u} = 1$, u =1,2,3, v=1,2,3. This corresponds to zero translation and no rotation.

B. Iterations:

1) For each point p_i (i=1, ... , N_p) of the scene **P**, compute the closest point $m_j \in \mathbf{M}$ from the model using the Euclidian distance. Let $\hat{\mathbf{m}}_i$ be the point on **M** corresponding to the minimum distance to p_i.

2) Using the selected correspondence pairs, compute the transformation, rotation (**R)** and translation (**T**), that minimizes the mean square error (MSE) of the estimated correspondence pairs:

$$\mathrm{MSE} = \frac{1}{\mathbf{N_p}} \sum_{\mathbf{i}=1}^{\mathbf{N_p}} \left\| \hat{\mathrm{m}}_{\mathbf{i}} - \mathbf{R}(\mathrm{p}_{\mathbf{i}}) - \mathbf{T} \right\|^2 . \quad (2)$$

Different close-form solution techniques of the original ICP algorithm can be used, i.e., quaternion (Horn, 1987; Mukundan, 2002) or single value decomposition (Arun et al., 1987).

The resulting transformation from the minimization of the above equation at step k will be denoted $\mathbf{R}_k$ and $\mathbf{T}_k$. This step also provides the minimum distances which correspond to the matched pairs.

3) Compute $\mathbf{P = R_k \times P_0 + T_k}$ and restart a new iteration if the change in the MSE is above a predefined threshold ζ, and if the maximum number of iterations $\mathbf{k}_{max}$ is not reached. If not, stop the iterations and exit.

2.2. PICP specifications

The PICP is similar to the OICP as it manipulates the correspondence search vectorially. A method of rejecting duplicate points is added to the first step of the OICP algorithm:

1a) For each point p_i (i=1, ... , N_p) of the scene **P**, compute the closest point $m_j \in \mathbf{M}$ from the model using the Euclidian distance. Let $\hat{\mathbf{m}}_{\mathbf{i}}$ be the point on **M** corresponding to the minimum distance to p_i,

1b) Among the resulting corresponding pairs, if more than one scene point p_i is assigned to the same model point m_j, then select p_i that corresponds to the minimum distance.

3. THE PROPOSED CICP ALGORITHM

In previous variants of the OICP algorithm, the search procedures for corresponding pairs of points are based on a line-by-line (vector) search within a **P**-**M** distance matrix described in Table 1, where

$d_{i,j}$ is the distance between p_i and m_j. Duplicate matches may hence occur, since multiple m_j (columns) can be assigned to different p_i (lines). The PICP variant ensures unique matches by rejecting all duplicate pairs, except the one with the smallest distance. This can be described as a line-by-line followed by a column-by-column search within the **P-M** distance matrix. Unfortunately, this may lead to the exclusion of good markers from the estimation procedure. To overcome this drawback, a more comprehensive search is needed.

A novel effective evaluation metric is introduced for correspondence search, called comprehensive lookup matrix measure. This measure ensures that ***every*** selected point on the scene surface has a ***unique*** match in the reference surface.

Table 1: The P-M distance matrix in which the Euclidian distance ($d_{i,j}$) between each scene point (p_i) and every model point (m_j) is calculated.

	m_1	m_2	…	m_{Nm}
p_1	$d_{1,1}$	$d_{1,2}$		$d_{1,Nm}$
p_2	$d_{2,1}$	$d_{2,2}$		$d_{2,Nm}$
:				
p_{Np}	$d_{Np,1}$	$d_{Np,2}$		$d_{Np,Nm}$

The CICP is different in that it sorts the $d_{i,j}$ distances in ascending order within the entire **P-M** distance matrix. Moreover, the point m_j is not considered to be a correspondence to p_i if either m_j or p_i has been previously assigned a correspondence. This ensures that each point in the scene surface will have a different association in the reference surface.

The CICP is the only ICP algorithm that makes use of all scene points in the search procedure to find the best and unique correspondence pairs. In other words, the **P-M** distance matrix is introduced to comply with the fact that a rotation is a bijective (one to one) function. Previous ICP implementations are based on vector not matrix analysis of the assignment problems. In this case, some elements in **M** may be mapped by more than one element in **P**, yielding surjection correspondences and incorrect estimations of rotation parameters. When the number of points in the two sets to be registered is not the same, the CICP algorithm considers the one with a smaller number

of points as a scene data set to ensure bijectivity of the resulting correspondence pairs. To reduce the computation time introduced by the matrix search procedure, matrix to vector conversion or fast assignment algorithms are used. The CICP algorithm replaces step 1 of the OICP algorithm by:

1) For each point $p_i \in \mathbf{P}$, (i=1, ..., N_p), the algorithm computes the Euclidian distance $d_{i,j}$ to each point $m_j \in \mathbf{M}$, (j=1, ..., N_m). Then, for N_p times, the algorithm:
   a. looks for the location (i,j) that corresponds to the minimum distance $d_{i,j}$ in the current look up matrix,
   b. assigns p_i to m_j as a correspondence pair,
   c. removes this correspondence pair from future consideration by eliminating the i^{th} row and j^{th} column.

Instead of leaving the decision of rejecting worse pairs till the end of each iteration as in (Zinsser et al., 2003), the CICP algorithm makes such a decision at the end of every selection of correspondence pairs. In addition to improving the rotation parameters estimation, such an approach improves the accuracy and the convergence of the ICP algorithms, as shown in the following sections.

4. ESTIMATION OF TRANSFORMATION PARAMETERS USING QUATERNION

For comparison reasons, the method presented in the OICP algorithm (Besl and McKay, 1992) for the estimation of the transformation parameters is used for the other two candidates. Following this method, rotation is expressed by a unit quaternion, $\vec{q}R = [q_0 \; q_1 \; q_2 \; q_3]^t$, and translation is expressed by a vector $\vec{q}T = [q_4 \; q_5 \; q_6]^t$. A rigid transformation can then be constructed by the two vectors: $\vec{q} = [\vec{q}R \,|\, \vec{q}T]^t$ which is no longer a quaternion but a vector in $\Re^7$.

Assuming that $\hat{M}_k$ is the rearranged reference data set obtained from the closest point research step:

- both $\mathbf{P}_k$ and $\hat{M}_k$ data sets have the same number of points (N_p),

- point correspondences are known, which means that for each iteration i, the point p_i corresponds to point $\hat{m}_i$ of the iteration k.

The anti-symmetric matrix is then formulated using the cross covariance matrix $\Sigma^{(k)}$ of the $\mathbf{P}_k$ and $\hat{M}_k$:

$$A^{(k)} = \Sigma^{(k)} - \Sigma^{(k)^t}. \tag{3}$$

where $\Sigma^{(k)} = \frac{1}{N_p}\sum_{i=1}^{N_p}\left[(p_i - \mu_p)(\hat{m}_i - \mu_{\hat{m}})^t\right]$, μ_p and $\mu_{\hat{m}}$ represent the center of mass of the scene data set $\mathbf{P}_k$ and the corresponding reference data set $\hat{M}_k$.

The elements of the anti-symmetric matrix are then used to construct the following matrix:

$$Q_k = \begin{bmatrix} tr(\Sigma_k) & \Delta^t \\ \Delta & \Sigma_k + \Sigma_k^t - tr(\Sigma_k) I_3 \end{bmatrix}. \tag{4}$$

where $\Delta = [A_{23} \;\; A_{31} \;\; A_{12}]^t$, A_{uv} is the u^{th}, v^{th} element of matrix A, and I_3 is a 3×3 identity matrix.

The optimal rotation is hence determined by calculating the eigenvector $qTr_k = [q_0 \; q_1 \; q_2 \; q_3]^t$ that corresponds to the maximum eigenvalue of the matrix Q_k. The rotation matrix can then be formulated as follows:

$$Tr_k = \begin{bmatrix} q_0^2 + q_1^2 - q_2^2 - q_3^2 & 2(q_1 q_2 - q_0 q_3) & 2(q_1 q_3 + q_0 q_2) \\ 2(q_1 q_2 + q_0 q_3) & q_0^2 + q_1^2 - q_2^2 - q_3^2 & 2(q_2 q_3 - q_0 q_1) \\ 2(q_1 q_3 - q_0 q_2) & 2(q_2 q_3 + q_0 q_1) & q_0^2 + q_1^2 - q_2^2 - q_3^2 \end{bmatrix}. \tag{5}$$

Finally, the optimal translation vector is calculated based on the obtained optimal rotation:

$$qTt_k = \mu_{\hat{m}} - Tr(qTr_k)\mu_p. \tag{6}$$

5. PERFORMANCE ANALYSIS

In this paper, the new CICP algorithm will be compared to the OICP and PICP. The PICP algorithm has been chosen as a benchmark since it is the only algorithm that addresses point to point

assignment (bijectivity) by discarding duplicate matching points. The robustness of the CICP algorithm will be studied under the presence of noise, with both synthetic and real medical data.

5.1. Noise generation

Real data are usually corrupted by noise caused by a wide range of sources, e.g. detector variations, environmental variations, transmission or quantization errors, etc. Here, the performance of the selected ICP algorithms is investigated under the effect of Gaussian and impulsive noise. In order to test the performance of the different algorithms in terms of estimating transformation parameters for the registration of surfaces affected by noise, noise is added to the scene data and then a known transformation (to be recovered) is applied.

5.1.1. Gaussian noise

Gaussian noise is added to the original data by the following method:

1) Transform all points of the data set from Cartesian to spherical coordinates (notations are shown on Figure 1):

$$p_i(x, y, z) \rightarrow \rho_i(\theta, \varphi) \quad \forall\, i = \{1, \ldots, N_p\}. \tag{7}$$

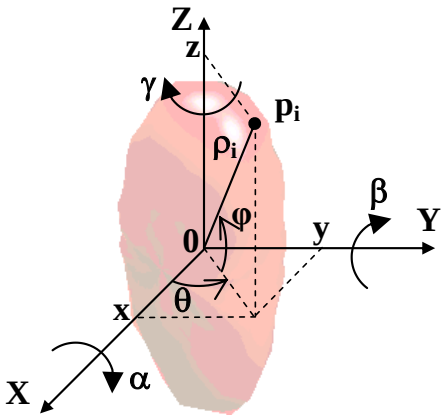

Figure 1: Cartesian to spherical coordinates transformation of star-like shape closed surfaces.

The transformation can be carried out without over determination for star-like shape closed surfaces where every radius launched from the origin crosses the surface in only one point. This is the case for medical closed surfaces used here for validation, as indicated on Figure 1.

2) Add noise to each resulting $\rho_i \; \forall$ i= {1, …, N_p} :

$$\rho_i = \rho_i + | \rho_i - \mu_\rho | \times 10^{-\mathbf{SNR\_dB}/20} \times \text{rand}(.) \tag{8}$$

where $\mu_\rho = \frac{1}{N_p} \sum_i^{N_p} \rho_i$, rand(.) is a random Gaussian number generator with mean zero and variance one, and **SNR_dB** is the required signal to noise ratio in dB.

3) Transform points back to Cartesian coordinates.

5.1.2. Impulsive noise

Impulsive noise is commonly referred to as outliers. In this case, a set of *h*% of the data points is assumed to be corrupted by impulsive noise. To generate outliers, replace step 2 of Gaussian noise generation by:

2a) Randomly selecting *h*% of the total data points.

2b) Modifying each selected point: $\rho_j \; \forall$ j= {1,..., $N_p \times h$ /100}

$$\rho_j = \rho_j \times (1+\beta) \tag{9}$$

where β represents the distribution of the outliers relative to the points of the original data set.

5.2. Performance parameters

To compare the performance characteristics of the CICP algorithm to OICP and PICP algorithms, three parameters are taken into consideration: the mean square error (MSE) between the registered data sets, the percentage of correct matches and the influence of differently sampled meshes.

5.2.1. Mean square error

The convergence property of the algorithm can be estimated by computing the mean square error (MSE) between the reference and the registered data sets, at each iteration of the algorithm. Since the

orientation is usually not known for both registered surfaces, the MSE can be computed by moving from Cartesian to spherical coordinates. When elements of the resulting 2D mesh have no data because of the resampling introduced by the Cartesian to spherical coordinates conversion, surface completion methods are applied to estimate the missing data (for example the method previously proposed by (Almhdie et al., 2004)).

In this paper, the MSE is considered as an error metric. It is computed as the mean square difference between the corresponding elements of the resulting 2D regular meshes obtained after conversion to spherical coordinates of the two reference and scene closed surfaces. This choice is imposed by the medical application that usually tends to minimize the distance between the two registered surfaces. Whereas the CICP calculates global MSEs, i.e, mean square error between the two surface data sets, the OICP and PICP calculate local MSEs, i.e., mean square error between estimated corresponding points. Therefore, making comparisons based on local MSE (Zinsser et al., 2003) is not valid since not all the points are always taken into consideration.

5.2.2. Percentage of correct matches

Correct matches analysis can be carried out only when the exact orientation of the two data sets to be registered is known, e.g. for validation purposes using simulated or known data. Under such a hypothesis, the percentage of correct associations of corresponding points from the scene and reference surfaces is counted at each step of the algorithm. Since each $p_i \in \mathbf{P}$ is a transformed point of $m_j \in \mathbf{M}$, then an association is defined as "correct" when j = i, that is to say $m_i = \hat{m}_i$ is assigned to p_i. This measurement is a straightforward indicator of the performance of the correspondence pair search method, as it reflects the quality of the correspondence pair estimation.

5.2.3. Influence of differently sampled meshes

In many classical situations, the size of the measured data (scene) and the size of the model data (reference) are different. Situations where the scene data are composed of a subset of the reference

data are tested here to evaluate the influence of sampled meshes of different sizes on the performance of the three ICP algorithms. The performances are compared by considering the number of iterations needed for the three ICP algorithms to converge.

6. CICP ALGORITHM EVALUATION

The CICP algorithm was tested under a noise-free situation as well as with Gaussian noise (with SNR of 10 dB and 20 dB) and outliers (with percentage of outliers of 10%, 15% or 20 % of the data set) conditions. The convergence properties and the accuracy of the proposed CICP algorithm have been evaluated using a real medical data set, since it is hard to find standard test data in the literature to compare performances of methods.

6.1. Material

The experiment considers a set of 922 points of real data of a human left lung as a reference surface (Figure 2a). The set of points is obtained from medical images acquired by perfusion scintigraphy, and is then transferred to a console for segmentation. The scene data set is simulated by rotating arbitrarily the reference scene data. The rotation was limited to 30° around the three main axes since the ICP algorithm is designed to refine rotation estimations of roughly registered data sets (for example, after computing the main inertia directions of each pair of data sets). In this experiment, results are chosen using a rotation of –29°, –4° and +8° around the x-axis, y-axis and z-axis, respectively (Figure 2b). To evaluate the repeatability of the results obtained using the left lung scene data, thirty other randomly selected rotations were applied on the reference data; the results obtained were equivalent to those presented below. The three OICP, PICP and CICP algorithms were tested to register the reference surface (Figure 2a) with the scene surface (Figure 2b), corrupted with Gaussian (Figure 2c) and outlier noise (Figure 2d). In order to compare the convergence and stability of the algorithms, here, the MSE threshold does not stop the iterative procedure and the maximum number of iterations is set to 100. The number of points in the reference and scene data sets is equal.

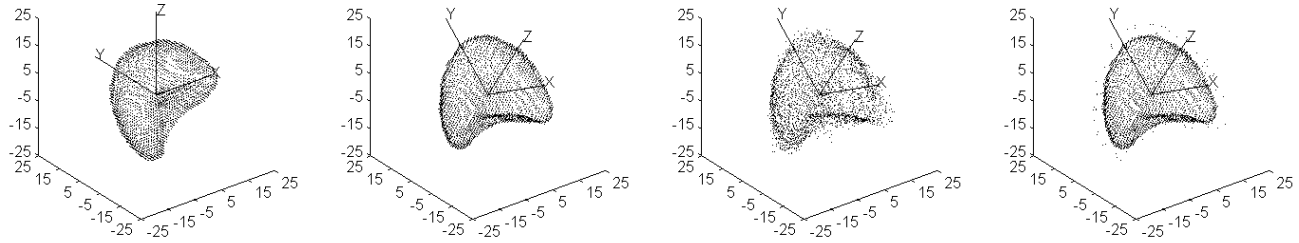

(a) **(b)** **(c)** **(d)**

Figure 2. Left lung data: a) Reference surface, b) Scene surface (rotation –29°, –4° and 8° around the x-axis, y-axis and z-axis, respectively, noise free), c) Scene surface (rotation, 10 dB Gaussian noise), d) Scene surface (rotation, 5% outliers).

6.2. Gaussian noise influence

The MSE between the reference and registered surfaces is measured at each iteration of the OICP, PICP and CICP algorithms, considering scene surface (Figure 2b) degraded with Gaussian noise (Figure 2c). In all the Gaussian noise tests, the MSE_O value represents the mean square error between the reference surface and the scene surface prior to applying the known transformation that will be estimated using the registration procedure. It is used as a performance indicator of the comparison. Table 1 presents some numerical results of the performance of the three algorithms at convergence. The first row of the table indicates the number of iterations reached at convergence, i.e., when the MSE error between the two registered surfaces becomes stable. The second row presents the percentage of points of the scene and reference surfaces that match correctly at convergence. Finally, the last row gives the computation time (expressed in seconds) needed to reach convergence. Numerical results are provided for values of SNR set respectively to 10 and 20 dB (columns 2 and 3), and for noise free data (column 4). For each noise situation, the values obtained with the CICP, PICP and OICP algorithms are provided.

Table 1: Performance results at convergence (left lung data, Gaussian noise)

	SNR= 10 dB			SNR= 20 dB			Noise free		
	CICP	PICP	OICP	CICP	PICP	OICP	CICP	PICP	OICP
Max. # of iterations	16	32	23	15	28	22	15	26	21
% of correct matches	90.8	84.2	85.5	99.3	99.2	99.5	100	100	100
Computation time (s)	35.9	28.1	24.2	33.2	25	23	25.5	16.5	16.7

Table 1 shows that the CICP algorithm converges faster in terms of number of iterations, even though the search procedure is more complex for the CICP than for the OICP and PICP algorithms. Due to the complexity of the search procedure, the duration of one iteration is longer for the CICP algorithm than for the other ones. Nevertheless, the reduction in the number of iterations yields a global computation time of the same order for the CICP algorithm.

6.2.1. MSE comparison

Figure 3 shows the evolution of the mean square error computed at the end of each iteration of the OICP, PICP and CICP algorithms. In this figure, the horizontal lines represent the MSE values (for SNR of 10 dB and 20 dB and noise free situations) between the two data sets before applying the transformations whose parameters are estimated by the three variants of the ICP registration algorithm. Under a noise free situation, the CICP algorithm approaches the pre-known MSE_O in a fewer number of iterations, compared to the OICP and PICP algorithms. Similar results are obtained for 10 and 20 dB amounts of Gaussian noise on the scene data. In all scenarios, although the search of correspondence points within the CICP is computationally expensive, it needs a much lower number of iterations to converge. In addition, the CICP approaches the MSE_O closer than the OICP and PICP algorithms. At SNR of 10 dB, we note that the CICP algorithm gives a better approximation to the mean square error between the two data sets before and after registration. The OICP and PICP algorithms, however, give lower MSE values at the end of the iterative process. This situation which could seem profitable at first approximation, corresponds to a particular configuration of the noise on the original data.

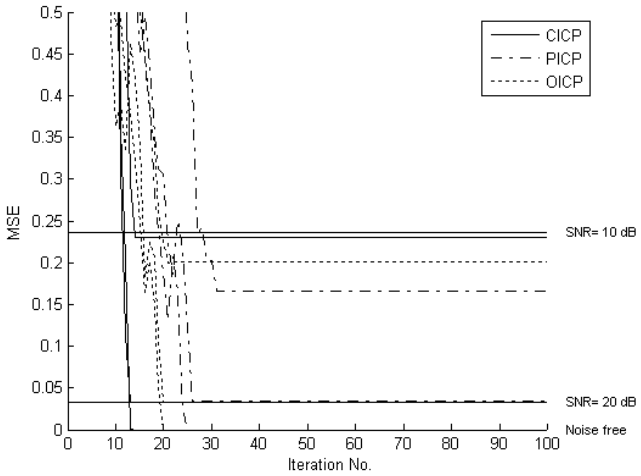

Figure 3. Left lung data registration, convergence comparison in the case of Gaussian noise. Solid horizontal lines represent MSE_0 values.

6.2.2. Correct matches evaluation

Figure 4 shows the percentage of correct matches at each iteration of the OICP, PICP and CICP algorithms. It can be seen that the CICP gives the highest number of correct matches, in fewer iterations, compared to both OICP and PICP algorithms, for the Gaussian noise situation tests undertaken. As the signal to noise ratio decreases, this superiority in achieving more correct matches becomes even clearer.

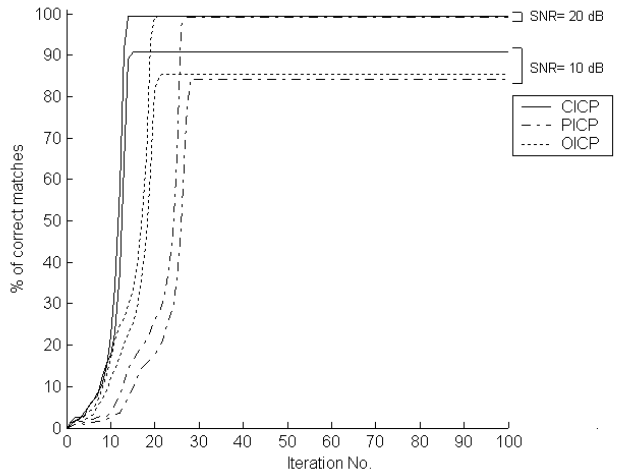

Figure 4. Left lung data registration, accuracy performance with 10 and 20 dB Gaussian noise addition.

6.2.3. Influence of differently sampled meshes

To test the behavior of the algorithms when the reference and scene surfaces contain a different number of points, the scene data are constructed as a partial set of the reference left lung data, selecting randomly from 70 % to 100 % of the reference data. The scene data are assumed to have been degraded by a Gaussian noise of SNR of 10 dB. Figure 5 shows that the CICP always converges faster than the other two algorithms in terms of number of iterations. As the PICP algorithm uses only the correspondence search part of the Picky ICP, the results presented here do not reflect the performance of the complete version of the Picky ICP, which is assumed to perform better than the OICP algorithm. However, the partial version of the Picky ICP has been used for comparison since it is known as a method that addresses duplicate assignment problems.

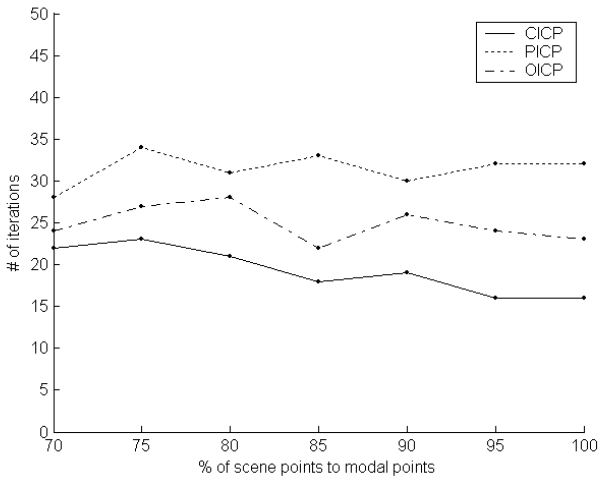

Figure 5. Left lung data. Number of iterations at convergence stage as a function of the rate of the scene data set number of points over the reference data set number of points (considering data corrupted with 10 dB Gaussian noise).

6.3. Impulsive noise influence

This section presents results for the case of scene data corrupted with impulsive noise. Table 2, constructed similarly to Table 1, reports the numerical results of the OICP, PICP and CICP algorithms when convergence is reached.

Table 2: Performance results at convergence (left lung data, impulsive noise).

	Outliers= 10 %			Outliers= 15 %			Outliers= 20 %		
	CICP	PICP	OICP	CICP	PICP	OICP	CICP	PICP	OICP
Max. # of iterations	17	29	22	16	30	23	17	31	21
% of correct matches	96.5	92.6	92.8	95	89.2	89.8	91.4	84.1	85.2
Computation time (s)	26.5	16.6	14.3	24.9	17.2	15	26.7	17.5	13.7

6.3.1. MSE comparison

Figure 6 presents the convergence property of the three algorithms in the presence of outliers. The CICP shows a good resilience to outliers even without adding a point rejection mechanism as introduced with the PICP algorithm. As with the results obtained with Gaussian noise, the CICP algorithm reaches convergence in fewer iterations than the other algorithms evaluated. It also approaches closer the pre-known MSE_O. This result indicates that the error between the two registered surfaces at the final stage is reduced with the new CICP algorithm.

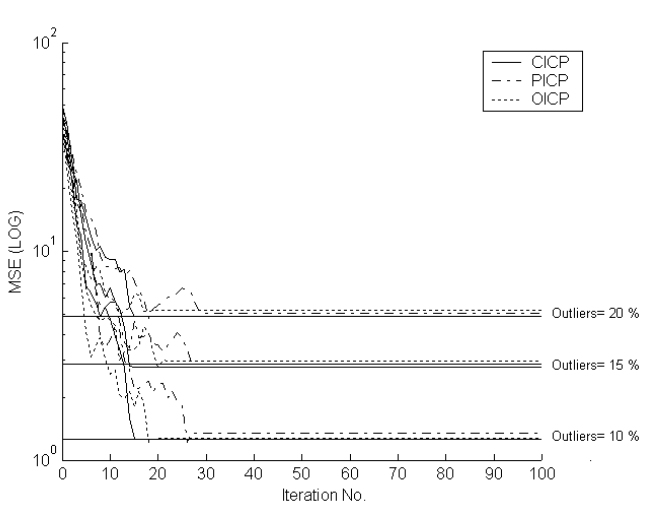

Figure 6. Left lung data registration, convergence comparison in the case of impulsive noise. Solid horizontal lines represent the MSE_O value.

6.3.2. Correct matches evaluation

The results presented in Figure 7 for the case of impulsive noise show the superiority of the CICP algorithm in finding higher correct associations of corresponding points of the scene and reference surfaces. One can note that the number of correct matches found with the CICP algorithm in the case of 15 % of outliers is greater than the number of correct matches obtained with the PICP and OICP algorithms in the case of only 10 % of outliers.

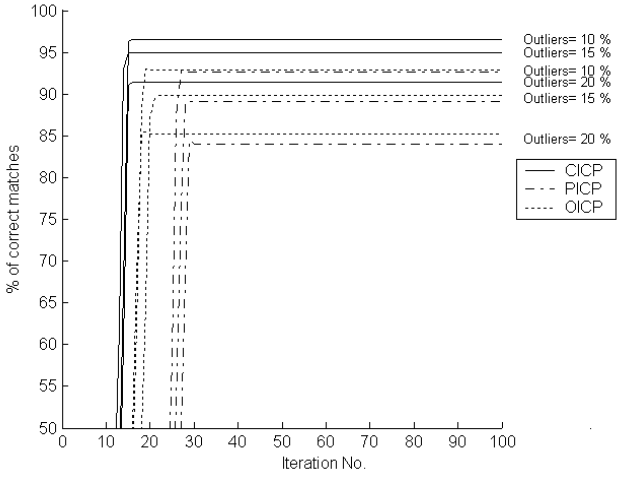

Figure 7. Left lung data registration, accuracy performance in the case of impulsive noise.

6.3.3. Influence of different sampled meshes

The results presented in Figure 8 are related to situations where the number of scene data points (corrupted by 20 % of impulsive noise) is reduced compared to the number of reference data points. The CICP algorithm needs fewer iterations than the other two algorithms to reach convergence. This is observed whatever the percentage (between 70 % and 100 %) of the number of points of the reference data set used to build the scene data set. In comparison with the OICP algorithm, the reduction factor in terms of number of iterations oscillates from 1.4 to 1.8.

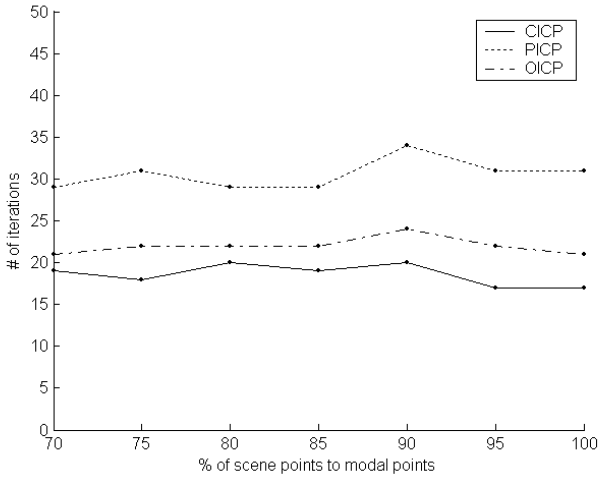

Figure 8. Left lung data. Number of iterations at convergence stage as a function of the rate of the scene data set number of points over the reference data set number of points (considering data corrupted with 20 % of outliers).

7. MULTIMODAL MEDICAL DATA REGISTRATION

Two experiments are reported in this section. The first one considers the registration of the left lung surface presented previously with a reference atlas of the left lung. The second test consists in registering two sequences of eight surfaces of the left ventricle of the heart, acquired from two different medical imaging modalities.

7.1. Left lung surface to reference atlas

In this experiment, the scene surface corresponds to the real left lung data shown in Figure 2a. The reference surface is a lung atlas obtained by segmenting manually under physician supervision the left lung of data provided by the Visible Human Project (creation of complete, anatomically detailed, three-dimensional representations of a male human body from transverse CT images of one millimeter intervals). The atlas data set consists of 1150 points, compared to the scene left lung data composed of 922 points. The motion parameters that "best" align the lung data set with the atlas are estimated using the three OICP, PICP and CICP algorithms. The corresponding registered data are displayed in Figure 9.

For the experiment carried out, the MSE threshold ζ between the reference surface and the registered scene surface is set to a low value (10^{-3}), and the maximum number of iterations ($k_{\max}$) is not limited. This ensures that the estimation of the motion parameters is reached. The algorithm stops when the estimated motion parameters are constant within several iterations. With lung atlas and lung data, the CICP, PICP and OICP algorithms achieve convergence in 31, 135 and 84 iterations, respectively, and the elapsed time is 72.9, 127.2 and 93.4, respectively. In this case, even though the computation time per iteration is higher for the CICP algorithm, the reduction in the number of iterations yields a global reduced computation time compared to the OICP and PICP algorithms.

In Figure 9, after stability of transformation parameters is reached, the CICP algorithm (Figure 9d) gives a better registration of the two data surfaces (Figure 9a), compared to the OICP (Figure 9b)

and PICP (Figure 9c) algorithms. This qualitative result was confirmed by a physician, expert in the field of medical imaging. Further experiments will be conducted to quantify these preliminary results precisely.

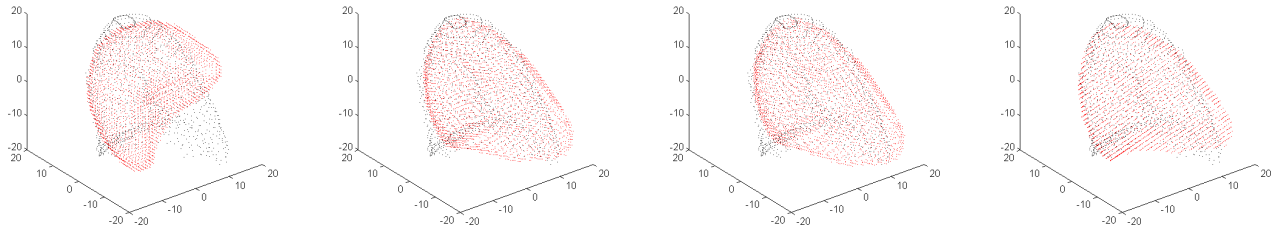

(a) **(b)** **(c)** **(d)**

Figure 9. Initial views: lung atlas (reference surface, black) and lung data (scene surface, red). Registered data using (b) OICP, (c) PICP, (d) CICP algorithms.

7.2. Sequences of the left ventricle of the heart

In this experiment, data consist of two sequences of eight surfaces of the left ventricle (LV) of the heart reconstructed within a cardiac cycle. Examinations were carried out on the same patient using successively two medical imaging modalities within a short period of time, in order to assume the LV deformations to be reproducible and hence medical comparisons applicable. The first sequence is composed of eight LV surfaces obtained after automatic segmentation from nuclear medicine imaging (NMI), known to be a “gold standard” examination for cardiac observation (Figure 10 a). The second LV sequence is provided by a new multidimensional ultrasound technique (US) called LV4D for Left Ventricle in 4 Dimensions (Bonciu et al., 2001) (Figure 10 b). The objective is to use the NMI examination to validate the new ultrasound method. The evolution of the NMI and US LV volumes as a function of time provides a global comparison of the reconstructed surfaces, as shown on Figure 11. Such figures have been used previously to compare globally the LV surfaces reconstructed using the two modalities. Experiments were carried out with data obtained on a patient with a pacemaker (Debrun et al., 1999) and on a mechanical phantom (Debrun et al., 2005), in order to ensure heart beat regularity and volume deformation reproducibility. However, the lack of

registration does not allow local comparisons, since the two surface absolute orientations are not known.

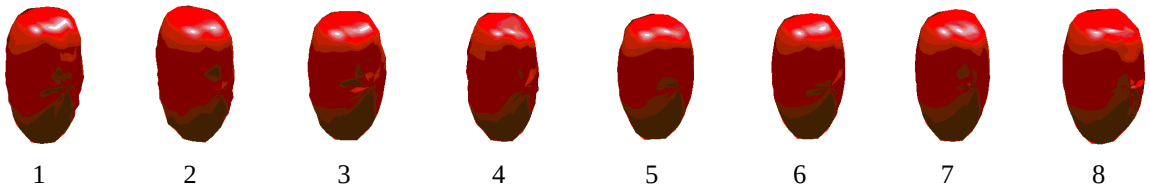

(a): Nuclear Medicine Imaging LV surfaces (reference data).

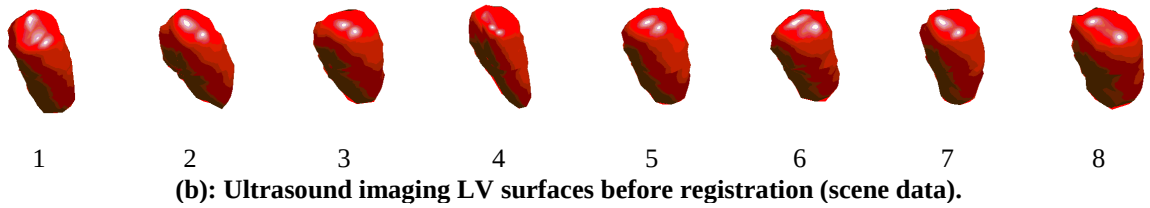

(b): Ultrasound imaging LV surfaces before registration (scene data).

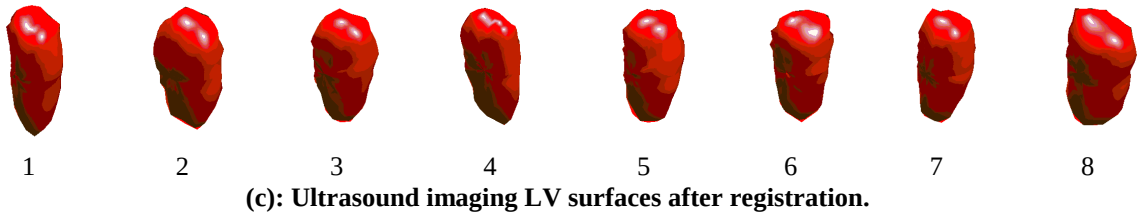

(c): Ultrasound imaging LV surfaces after registration.

Figure 10. Registration of two sequences of eight LV surfaces acquired from Nuclear Medicine and Ultrasound imaging.

Even though the patient relative orientation varies inevitably between NMI and US examinations, it is reasonable to consider that it remains the same relative to an absolute reference system of coordinates during each examination. Thus, the transformation parameters to be estimated are expected to be equivalent for all registered pairs of the corresponding surfaces. Differences in parameter values may occur because of the noise level that alters data, usually with a significant ratio in medical imaging (due for example to the resolution of the imaging techniques, the quality of the segmentation algorithms that produce surfaces, etc.).

Table 3 indicates the (α,β,γ) Euler angle values (columns 2 to 9), estimated using the CICP algorithm with the eight NMI and US LV volumes shown in Figure 10a and Figure 10b. The last two columns (10 and 11) give the mean and standard deviation of the eight corresponding angle estimations. The results obtained for each pair of surfaces are globally coherent, except for the γ Euler angle.

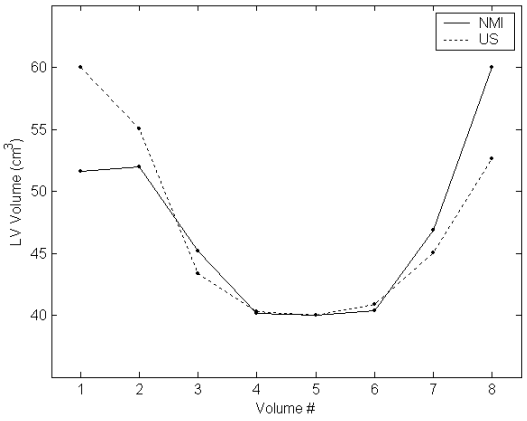

Figure 11. Global comparison of NMI and US left ventricular volumes, delineated by the closed surfaces shown in Figure 10 (a and b), within a cardiac cycle.

α and β angles are evaluated correctly (μ_α = 20.4, σ_α = 3.0, μ_β = 6.8, σ_β = 6.3, respectively) since estimating the rotation angles around the X and Y axes is relatively straightforward for LV shapes (refer to Figure 1 for notations). On the contrary, the γ angle is found with a high degree of incertitude (μ_γ = 2.0, σ_γ = 21.0), yielding non significant γ estimations without further study. This result is due to the shape of the LV, usually modeled by a semi-ellipsoid or a bullet, which presents a rotational symmetry around the Z axis and gives undefined γ angle values. Some shape discontinuities (observed for pathological cases such as ischemia, left ventricle shape irregularities, local deformations due to the right ventricle influence, overdeveloped papillary muscles, etc.) might be helpful in estimating the γ angle. Moreover, signal-post processing can be applied on the available γ angle values in order to refine coarse estimations. In this case, more than eight different γ estimations would certainly be a prerequisite.

Table 3: The estimated Euler angles used as rotation parameters for the registration of left ventricular surfaces reconstructed using NMI and US medical imaging modalities.

Volume #	**1**	**2**	**3**	**4**	**5**	**6**	**7**	**8**	**μ**	**σ**
α	20.7	17.9	21.7	16.2	21.1	25.4	17.7	22.4	**20.4**	**3.0**
β	10.2	20.2	6.9	2.0	1.1	0.9	7.0	6.5	**6.8**	**6.3**
γ	-23.2	47.3	-11.5	-8.3	2.1	11.9	-2.2	0.2	**2.0**	**21.0**

8. CONCLUDING REMARKS

In this work, a novel enhanced implementation of the ICP algorithm is presented. The use of the complete look-up distance matrix during the point association procedure guarantees that unique matches are obtained for all points from the scene data. The substitution of a vector by a matrix based search of correspondence pairs ensures correct transformation parameter estimation used for rigid registration, in agreement with the bijective property of the rotation. Compared to other ICP implementations, the proposed CICP algorithm provides: a faster convergence, in terms of number of iterations, a more precise estimation of pair of points correspondence, and a better resilience to additive Gaussian noise and outliers. Even though all experiments carried out with the CICP show better convergence and stability than the other OICP and PICP reference algorithms, theoretical demonstration still remains to be developed. In addition to minimizing the number of ICP iterations, the computing time expansion due to the switch from vector to matrix search is limited. Improvements in computation time reduction are currently being investigated using valuable techniques known to solve assignment problems: LMedS (Least Median of Squares) estimator (Masuda and Yokoya, 1994), M-estimator (Trucco et al., 1999) and Minmax estimation (Jaulin and Walter, 2002). The accuracy of the proposed CICP has been investigated and promising results have been shown for 3D real medical data registration. This step is part of a more general research work aimed at comparing locally and validating quantitatively surfaces of star-like shape organs, reconstructed from different medical imaging modalities.

ACKNOWLEDGEMENTS

This work was partially sponsored by a grant from the *University of Sebha, Libya*. The authors would like to thank particularly Dr Fabienne Thérain and Dr Long-Dang Nguyen, from the *Nuclear Medicine and Cardiology Departments* of the *Regional Hospital Center of Orleans* for providing the medical data.

REFERENCES

Akca, D. (2004). "A New Algorithm for {3D} Surface Matching." Int. Archives of Photogrammetry, Remote Sensing and Spatial Information Sciences (ISPRS): 960-965.

Almhdie, A., Léger, C., et al. (2004). Smooth Surface Reconstruction from Sparse Data: Comparison of SVSF and 3DHM Algorithms. IEEE GCC 2004, Manama, Kingdom of Bahrain.

Arun, K. S., Huang, T. S., et al. (1987). "Least-squares fitting of two 3-D point sets." IEEE Transactions on Pattern Analysis and Machine Intelligence **9**(5): 698-700.

Audette, M. A., Ferrie, F. P., et al. (2000). "An algorithmic overview of surface registration techniques for medical imaging." Med Image Anal **4**(3): 201-17.

Bendels, G. H., Degener, P., et al. (2004). Image-Based Registration of 3D-Range Data Using Feature Surface Elements. The 5th International Symposium on Virtual Reality, Archaeology and Cultural Heritage (VAST 2004), Brussels and Oudenaarde, Belgium.

Besl, P. J. and McKay, H. D. (1992). "A method for registration of 3-D shapes." IEEE Transactions on Pattern Analysis and Machine Intelligence **14**(2): 239-256.

Bonciu, C., Weber, R., et al. (2001). "4D reconstruction of the left ventricle during a single heart beat from ultrasound imaging." Image and Vision Computing, Elsevier Eds **19**: 401-412.

Chetverikov, D., Svirko, D., et al. (2002). The Trimmed Iterative Closest Point algorithm. 16th International Conference on Pattern Recognition (ICPR'02)

Cuadra, M. B., Pollo, C., et al. (2004). "Atlas-based segmentation of pathological MR brain images using a model of lesion growth." Medical Imaging, IEEE Transactions on **23**(10): 1301-1314.

Debrun, D., Thérain, F., et al. (1999). "Mesure des volumes du ventricule gauche par échocardiographie 4D: résultats préliminaires sur la comparaison à la tomo-scintigraphie myocardique synchronisée." Médecine Nucléaire - Imagerie fonctionnelle et méthabolique **23**(2): 77-80.

Debrun, D., Thérain, F., et al. (2005). "Volume measurements in nuclear medicine gated SPECT and 4D echocardiography: validation using a dynamic cardiac phantom." The International Journal of Cardiovascular Imaging **21** 239-247.

Elsen, P., Pol, E., et al. (1993). "Medical Image Matching—A Review with Classification." IEEE Engineering In Medicine and Biology **12**: 26-39.

Horn, B. K. P. (1987). "Closed-form solution of absolute orientation using unit quaternions." Journal of the Optical Society of America **4**(4): 629-642.

Jaulin, L. and Walter, E. (2002). "Guaranteed robust nonlinear minimax estimation." Automatic Control, IEEE Transactions on **47**(11): 1857-1864.

Kagadis, G. C., Delibasis, K., et al. (2002). "A comparative study of surface- and volume- based techniques for the automatic registration between CT and SPECT brain images." Medical Physics **29**(2): 201-213.

Kneuaorek, K., Ivanovic, M., et al. (2000). "Medical Image Registration." Europhysics News **31**(4).

Liu, Y. (2004). "Improving ICP with easy implementation for free-form surface matching." Pattern Recognition **37**(2): 211-226.

Maintz, J. B. and Viergever, M. A. (1998). "A survey of medical image registration." Med Image Analysis **2**(1): 1-36.

Masuda, T. and Yokoya, N. (1994). A robust method for registration and segmentation of multiple range images.

Matabosch, C., Fofi, D., et al. (2005). Reconstruction et Recalage de Surfaces en Mouvement par Projection Laser Multi-lignes. ORASIS'05, Fournol, France.

Mukundan, R. (2002). Quaternions: From Classical Mechanics to Computer Proceedings of the 7th Asian Technology Conference in Mathematics (ATCM 2002), invited paper. Malaka, Malaysia.

Ourselin, S. (2002). "Recalage d'images médicales par appariement de régions : Application à la construction d'atlas histologiques 3D." INRIA, Thèse de : Nice - Sophia Antipolis.

Rusinkiewicz, S. and Levoy, M. (2001). Efficient variants of the ICP algorithm. Proceedings of the Third International Conference on 3-D Digital Imaging and Modeling., Quebec City, Quebec, Canada.

Sharp, G. C., Lee, S. W., et al. (2002). "ICP registration using invariant features." IEEE Transactions on Pattern Analysis and Machine Intelligence **24**(1): 90-102.

Sylvain, J. (2000). "Modélisation multi-résolution d'objets articulés pour le recalage et l'analyse d'images médicales." Rapport de recherche, FRIA, France.

Trucco, E., Fusiello, A., et al. (1999). "Robust motion and correspondence of noisy 3-D point sets with missing data " Pattern Recogn. Lett. **20**(9): 889-898

Wan, R. and Li, M. (2003). An overview of medical image registration. The Fifth International Conference on Computational Intelligence and Multimedia Applications (ICCIMA'03), Xi'an, China.

Zinsser, T., Schmidt, J., et al. (2003). A refined ICP algorithm for robust 3-D correspondence estimation. Proceedings of IEEE International Conference on Image Processing Barcelona, Spain.

Zitová, B. and Flusser, J. (2003). "Image registration methods: a survey." Image and Vision Computing **21**(1): 977-1000.